IEEE Photonics Journal
An IEEE Photonics Society Publication

Open Access

Manipulation of Random Lasing Action From Dye-Doped Liquid Crystals Infilling Two-Dimensional Confinement Single Core Capillary

Volume 7, Number 3, June 2015

Ja-Hon Lin
Ying-Li Hsiao
Bo-Yu Ciou
Sheng-Hung Lin
Yao-Hui Chen
Jin-Jei Wu

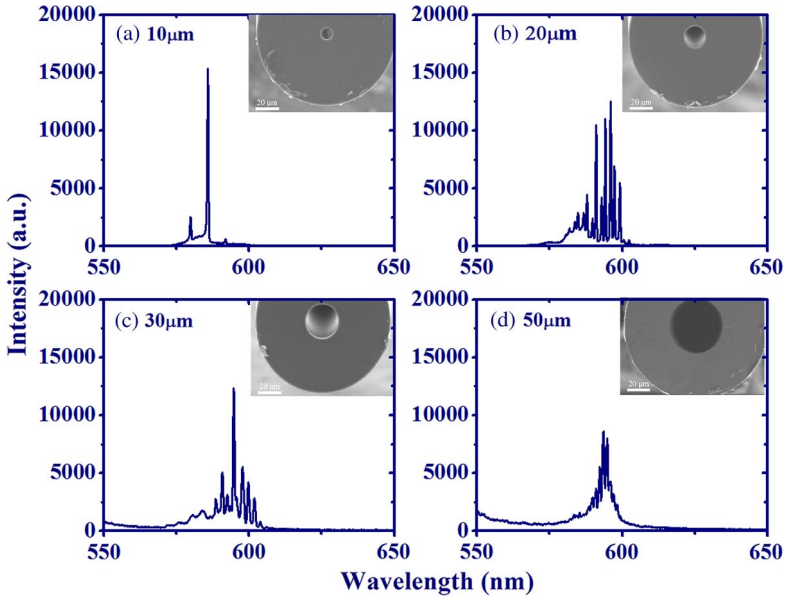

DOI: 10.1109/JPHOT.2015.2421441
1943-0655 © 2015 IEEE

Manipulation of Random Lasing Action From Dye-Doped Liquid Crystals Infilling Two-Dimensional Confinement Single Core Capillary

Ja-Hon Lin, Ying-Li Hsiao, Bo-Yu Ciou, Sheng-Hung Lin, Yao-Hui Chen, and Jin-Jei Wu

Department of Electro-Optical Engineering and Institute of Electro-Optical Engineering, National Taipei University of Technology, Taipei 10608, Taiwan

DOI: 10.1109/JPHOT.2015.2421441

Manuscript received March 3, 2015; revised April 2, 2015; accepted April 5, 2015. Date of publication April 10, 2015; date of current version April 29, 2015. This work was supported by the National Science Council of Taiwan under Grant NSC 102-2112-M-027-001-MY3. Corresponding author: J. H. Lin (e-mail: jhlin@ntut.edu.tw).

Abstract: The experimental detail of a random lasing action from dye-doped nematic liquid crystals (LCs) inside single-core capillaries with a core diameter below 50 μm was investigated. The resonant characteristics, including the number of emission spikes, the full width at half maximum (FWHM), and the estimated *Q*-factor, were shown to depend on the core diameter of a capillary. In contrast with a capillary with a larger core diameter and having various emission spikes, only three emission spikes were excited from a capillary with a 10-μm core diameter, owing to the smaller effective area of the pump beam. However, the decrease in the amplitude of emission spikes and the broadening of the linewidth accompanying the higher lasing threshold from a capillary with a 50-μm core diameter are attributed to the decrease in the pump fluence and the increase in the scattering loss, respectively. In this paper, a random laser (RL) with the shortest FWHM emission peak of about 0.47 nm and the highest *Q*-factor of about 1268 was generated from the capillary with a 20-μm core diameter. By means of temperature adjustment, the emission spectra of the RL that is related to the birefringence and alignment ordering of the LC molecules inside a capillary with a 20-μm core diameter can be effectively altered. Our experiments show that the RL, revealing adjustable output emission spectra, can be a promising device in using remote sensing applications.

Index Terms: Random lasing, dye-doped liquid crystals, single core capillary, recurrent multiple light scattering.

1. Introduction

Since the first proposition by Letokhov in 1968 [1], random lasers (RLs) have been theoretically predicted and experimentally investigated over the past several decades. Compared with traditional laser, RLs no need resonator and manifest some unique properties such as low spatial coherence, multiple emission lasing wavelengths, broad solid angle output emission, and compact cavity geometry. Therefore, RLs have opportunity to be used in several special issues like suppressing the speckle noise [2] and bio-medical diagnosis [3]. In order to produce RLs, it is crucial to immerse active media into tiny and disordered dielectric materials so

that emission light from gain medium might experience recurrent multiple scattering in the diffusive materials to induce photon localization or Anderson localization [4]. To date, a variety of materials such as ZnO powders [5], polymers [6], porous glass [7], and biological structure [8], [9] have been experimentally adopted for light scattering. As pump energy increases under the condition that accumulated gain exceeds loss, narrower coherent spikes are excited above the broadband spontaneous emission spectrum. In previous report, the characteristics of RLs including lasing threshold, the number of excited modes, and the linewidth of emission spikes are affected by the structure size of scattering materials [10], [11], excitation area of pump beam [12], [13], optical infilling factor [14] and some additional confinements [15]–[17]. For some experimental results, lasing threshold of RL was demonstrated to depend on the excitation beam radius and thus only a few localized modes were existed within the excitation area [12], [13]. Besides, pump threshold for RL was obviously decreased and slope efficiency was efficiently enhanced with the assistance of additional confinement such as one dimensional planar micro-cavity [15]. In other experimental study, 2-D confinement such as single core capillary or photonic crystal fiber has also been investigated in fluidic laser by infilling the toluene solution with organic dye to produce a serial emission peaks [16]. Using TiO_2 as the scattering medium suspended in rhodamine 6G solution within a hollow core photonic crystal fiber, more efficient RLs behavior was verified [17].

Because of the intrinsic birefringence, LCs reveal excellent light scattering property that has been used inside RLs. One of the most superior advantage, in comparison with other scattering materials, the output property of the dye-doped liquid crystal (DDLC) lasers can be easily controlled by the external modulation such as electric filed [18]–[20], magnetic field [21], optical irradiation [22], or temperature [23]–[25]. Experimentally, weak localization of light has been demonstrated by infiltrating the nematic liquid crystals (NLCs) within the glass cell [26]. Furthermore, light scattering can be greatly enhanced after curing the monomer in the LC mixtures to produce submicron- to micron-size droplet. Therefore, behavior of RLs has been reported in dye-doped polymer dispersed LCs (PDLCs) [27], [28]. With additional mixing of the silver or ZnO nano-particle into the dye-doped PDLCs, the further reduction of the lasing threshold was also approved [29], [30]. In contrast with former studies, additional scattering objects like polymer or nano-grains are cooperated with LCs to suppress light diffusion and cause light localization. In this work, we investigate the action of RL by infilling of dye-doped nematic liquid crystals (DDNLCs) into 2-D confinement single core capillaries with core diameters below 50 μm to force the alignment of LCs along the capillary. After excitation by the Q-switched laser, the characteristics of RLs including the number of emission spikes, estimated Q-factor and lasing threshold energy are apparently distinct at different core diameter capillaries that was attributed to the ordering of LCs alignment, excited area of the pump beam, and experienced scattering loss. Furthermore, we also demonstrate that the output emission spectra of the DDLCs inside capillary can be efficiently adjusted by means of temperature.

2. Sample Preparation and Experimental Setup

The DDLC mixtures were prepared by chosen NLCs (E7, $n_e = 1.7462$, $n_o = 1.5216$, $\Delta n = 0.2246$, clearing point around 70 °C) as main scattering materials and two distinct laser dyes, 0.5 wt% concentration Pyrromethene 597 (PM597, Exciton Inc.) and 4-(dicyanomethylene)-2-methyl-6- (4-dimethlyaminostryl)-4H-pyran (DCM, Exciton Inc.) as the active media. Then, the DDLC mixtures were placed in a small vessel which was heated by a hot plate to make the LCs transition to the isotropic phase. In addition, we continuously stirred admixture by using little glass rod to make sure fluorescent molecules uniformly dispersive within LCs. After immersing a 5 cm long single core capillary (TSP010150, Polymicro Technologies Inc.) into this vessel for a few days, the LC mixtures were filled into the hollow core through the capillary effect. To investigate the characteristics of RLs, we selected single core capillaries with four different core diameters of 10 μm (capillary *I*), 20 μm (capillary *II*), 30 μm (capillary *III*), and 50 μm (capillary *IV*), respectively, that were covered with 125 μm diameter fused silica cladding.

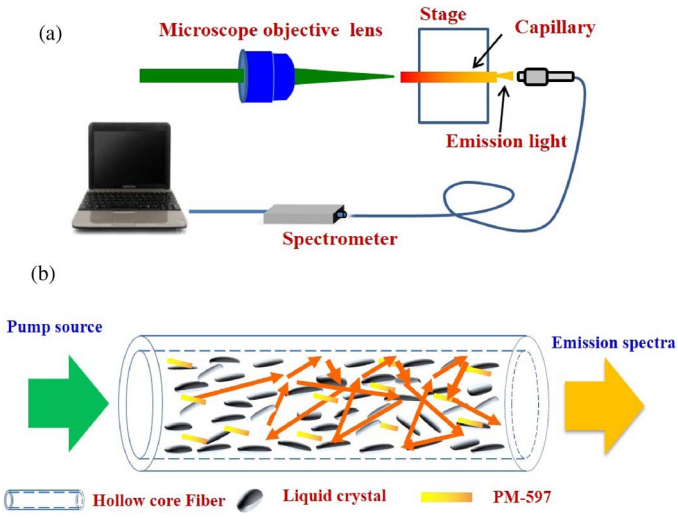

Fig. 1. (a) Schematic illustration of the experimental setup of RL from the DDLCs inside the single core capillary. (b) Description of the recurrent multiple light scattering inside the single core capillary comprising of the slightly disordering alignment of NLCs and fluorescent molecules.

As shown in Fig. 1(a), the DDLCs infiltrated single core capillary was clipped on a high-resolution 3-axis translation stage to ensure high coupling efficiency of pump beam. A frequency-doubling Q-switched Nd:YAG laser with central wavelength at 532 nm, 50 Hz repetition rate, and 2.2 ns pulse duration was used as an excitation source of RLs. After spatial beam expansion and collimation, the pump beam was coupled into the single core capillary through a 10x microscope objective lens. Due to higher average refractive index of E7 than glass fiber, pump beam and emission light from fluorescent molecules were guided within the core area of capillary. In this work, the effective area of excited beam and pump fluence inside the capillary are dominated by the core radius. Generally, a smaller excited area with higher pump fluence is produced in a smaller core diameter capillary. The emerged spectra from the single core capillary were collected by a fiber tip and then measured by the spectrometer with the resolution around 0.3 nm (Ocean Optics Inc.). The schematic illustration for the recurrences of multiple scattering lights within DDLCs inside single core capillary is shown in Fig. 1(b). As DDLC mixtures were filled into the single core capillary, the director of LCs would generally align along the axial direction of the single core capillary, but their positions were totally random. Owing to the intrinsic birefringence of the NLCs, the emission light from fluorescent molecules with different incident angle relative to the optical axis of LC would undergo different refractive index to cause multiple light scattering and form a closed loop, as well as constructive interference. At certain pump energy, the obtained gain of laser within DDLC mixtures inside capillary will exceed loss to produce narrow coherent spikes.

3. Results and Discussion

In Fig. 2, the blue dash and red dot curves represent the Photoluminescence (PL) emission spectra from PM597 and DCM, respectively, using the continuous wave (CW) green laser with central wavelength at 532 nm as an excitation source. In this figure, the bandwidth of PL emission from these two lasing dyes, PM597 and DCM, are relatively broad whose emission peaks are located at 583 nm and 615 nm, respectively. After excitation by the Q-switched laser with pulse energy of about 50 μJ/pulse, the stimulated emission spectra from a 20 μm core diameter capillary using 0.5 wt% PM597 (blue solid curve) or DCM (red solid curve) as gain medium are shown in Fig. 2. It is clear to see multiple emission spikes, with narrower linewidth below 1 nm, on the pedestal of the spontaneous emission spectrum that is one characteristic of RL. Unlike traditional laser whose emission wavelength is determined by the coating mirror, the multiple emission spikes from RLs are dominated by the gain spectrum of fluorescent molecule.

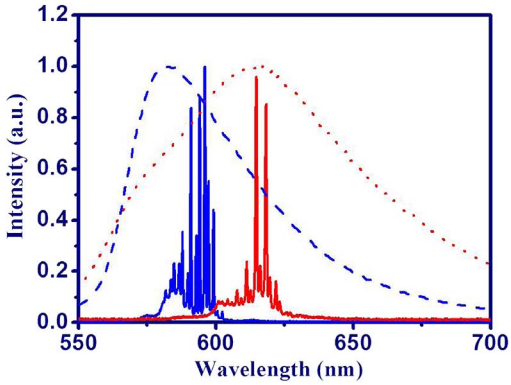

Fig. 2. Stimulated emission spectra from a 20 μm core diameter capillary infilling of PM597 (blue solid curve) or DCM (red solid curve) as gain medium. The blue dash curve and red dot curve represent the PL emission spectrum from PM597 and DCM, respectively.

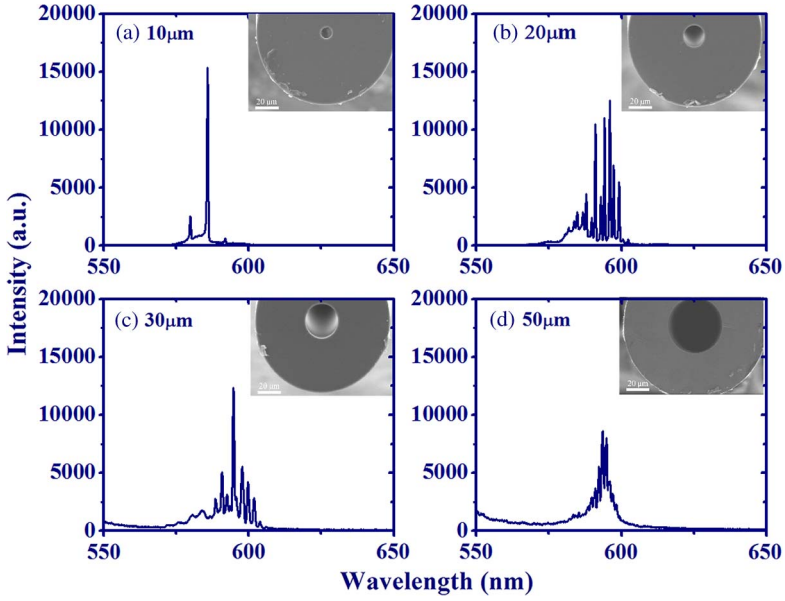

Fig. 3. Stimulated emission spectra from single core capillary infilling of laser dye (PM597) and NLCs (E7) with core diameter of (a) 10 μm, (b) 20 μm, (c) 30 μm, and (d) 50 μm, respectively, and the inset show the corresponding SEM images.

Therefore, the wavelength of maximum emission peak from the DDLCs inside the capillary using DCM (about 614.8 nm) as gain medium is longer than that using PM597 (about 588.6 nm).

Fig. 3(a)–(d) show the emerged lasing peaks from DDLC mixtures using PM597 as gain medium inside four different capillaries (capillary *I*, *II*, *III*, and *IV*) with core diameters of 10 μm, 20 μm, 30 μm, and 50 μm, respectively, under the same pump energy (50 μJ/pulse). The corresponding cross section of capillary from SEM images are also shown in the inset. In Fig. 3(a), three emission peaks were simultaneously excited within a 10 μm diameter capillary with the central wavelengths at 579.8 nm, 585.8 nm, and 591.8 nm, respectively. Theoretically, if the Fabry-Perot etalon resulting from the circumference of the hollow core plays the dominant role, it means that the accumulated phase shift $(\Delta\phi)$ for each loop requires to meet the condition:

$$\Delta\phi = \frac{2\pi}{\lambda} n_{eff} l = 2\pi m \tag{1}$$

TABLE 1

Peak wavelength (λ_p), FWHM and estimated Q-factor of emission spectrum from DDLC in the single core capillary with different core diameters

Core diameter (μm)	10(capillary I)	20(capillary II)	30 (capillary III)	50(capillary IV)
Peak wavelength (nm)	585.8	596.0	594.7	593.5
FWHM (nm)	0.52	0.47	0.64	0.95
Q-factor($\lambda_p/\Delta\lambda$)	1126.5	1268.1	929.1	624.8

where *l* is the path of the closed loop, $n_{eff} = (2n_o + n_e)/3$ is the effective refractive index of the NLCs, λ is the central wavelength of the lasing peak, and *m* is an integer. From (1), the wavelength spacing $(\Delta\lambda)$ of two adjacent longitudinal modes can be determined by using the formula:

$$\Delta\lambda = \frac{\lambda^2}{n_{eff} l}. \tag{2}$$

With the emission peaks shown in Fig. 3(a), the estimated path of the closed loop about 36.1 μm is larger than the practical core circumference length of 10 μm core diameter capillary (31.4 μm). When we chose the 20 μm core diameter capillary to increase effective pump area, more closed loops were excited so as to increase the number of emission spikes with unequally wavelength spacing as shown in Fig. 3(b). In addition, the decrease of frequency interval between two neighboring peaks accounts for the elongation of closed loop path. However, the estimated *l*, in choosing any two sequential peaks in Fig. 3(b), is almost twice length larger than the core circumference of capillary. This indicates that the fine structure of emission peaks from capillary does not result from the whispering gallery modes along the boundary of the hollow core.

However, the number of emission spikes diminishes and the intensity contrast between emission spikes relative to the amplitude of spontaneous emission decreases, as shown in Fig. 3(c) and (d), if we further increase core diameter to 30 μm and 50 μm, respectively. The reasons are attributed to the declining of pump fluence, the excited energy per effective area in the core regime, and the raising of scattering loss as the disordering of the LCs alignment in large core diameter capillary increases. Table 1 lists the peak wavelength (λ_p), Full-Width at Half-Maximum (FWHM, $\Delta\lambda$) and the estimated Q-factor $(\lambda_p/\Delta\lambda)$ of the highest emission spike in four different core diameters. It indicates that the capillary *II* (core diameter is 20 μm) has the shortest emission linewidth (FWHM) of about 0.47 nm and the highest Q-factor of about 1268. As core diameter increases to 50 μm, the measured FWHM increases to about 0.95 nm and the Q-factor declines to about 624.8.

In this work, we used the polarization optical microscopy (POM) to confirm the ordering of LCs alignment inside the capillary which was sandwiched between two cross polarizers (polarizer *I* and polarizer *II*) as shown in Fig. 4(a). The images of the optical microscopy (OM) from capillaries *II* and *IV* infilling of liquid crystals, without [see Fig. 4(a)] and with cross polarizer [Fig. 4(b)–(d)], are shown in Fig. 4. The clear structure of the capillary *II* including the central core and outer cladding is shown in the image of the OM, without using the other cross polarizer (polarizer *II*), as the capillary was placed in parallel to the polarizer *I*. After inserting the polarizer *II*, the image of POM from the capillary *II* became dark in Fig. 4(c). However, the POM image turned into bright while the capillary *II* was rotated 45° relative to each polarizer [see Fig. 4(d)]. It depicts that the arrangements of NLCs inside capillary are approximately along the axis direction of capillary because of the adhesion force between the LC molecules and the inner wall of capillary. Comparing to the capillary *II*, slightly brighter spots can be seen from the image of POM as the capillary *IV* was placed along the polarizer *I* [see Fig. 4(e)]. Owing to the decrease in the ratio of the contacted surface relative to the total volume of LCs inside a 50 μm core diameter capillary, the influence of the adhesion force decreases to cause more disordering alignment of the NLCs. In previous work [28], random lasing emission spikes do not appear from DDNLCs inside a glass tube with 110 μm inner diameter through pump by a frequency-doubling Q-switched Nd:YAG laser. It is recognized that light scattering decreases as the alignment of LCs become relatively random, and

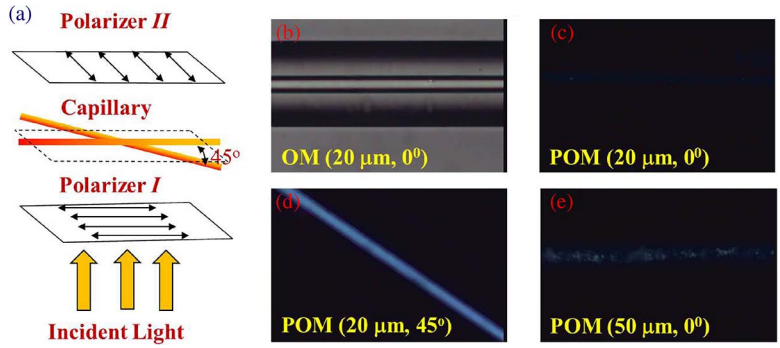

Fig. 4. (a) Schematic setup for the polarization optical microscopy (POM) measurement of the NLCs infilling capillary and (b) image of optical microscopy (OM) as the capillary *II* parallel to the polarizer *I*, (c) image of POM from capillary *II* with the insertion of crossed polarizer *II*, (d) image of POM as capillary *II* was rotated 45 °C relative to the polarizer *I*, and (e) image of the POM as the capillary *IV* parallel to the polarizer *I*.

thus, the birefringence property of LC disappeared. Therefore, the macro-property of LCs inside the capillary is like the isotropic state.

Fig. 5(a), (c), and (e) show the evolution of emission spectra from the capillaries *I*, *II* and *IV* (10 μm, 20 μm, and 50 μm core diameter) as the pump energy (E_p) increases from 10 μJ/pulse to 50 μJ/pulse. For the capillary *I* (10 μm core diameter), one emission spike with central wavelength at 585.8 nm [pink curve in Fig. 5(a)] could be excited at lower pump energy of about 10 μJ/pulse. As pump energy increased, the intensity of emission spike was amplified obviously but the amplitude of spontaneous emission did not vary apparently. With $E_p = 50$ μJ/pulse, two additional peaks with central wavelength at 579.8 nm and 591.8 nm, respectively, were excited as shown from black curve in Fig. 5(a). For the capillary *II* (20 μm core diameter), various tiny emission spikes with narrow FWHM were excited under pump energy of 10 μJ/pulse. Due to the re-absorption of the lasing dye, the emission spikes at longer wavelength regime would be amplified obviously than that at shorter wavelengths regime under higher pump energy [28]. The residual amplified spontaneous emission could be seen at shorter wavelengths. Fig. 5(e) reveals the evolution of the emission spectra versus the pump energy from capillary *IV* (50 μm core diameter) that indicates some different characteristics in comparison to previously two capillaries. Only spontaneous emission could be seen from capillary *IV* at lower excited energy. The emission spikes would be excited on the top of the spontaneous emission spectrum until $E_p = 20$ μJ/pulse. With further enhancement of the pump energy, not only the intensity of the emission spikes but also the spontaneous emission increases. Therefore, the intensity contrast of the emission spikes relative to the spontaneously emission spectrum is smaller in comparing to that shown in capillaries *I* and *II* with 10 μm and 20 μm core diameters.

The values of peak intensity (black solid squares) and FWHM (blue solid circles) of the emission spikes from capillaries *I*, *II*, and *IV* as a function of pump energy are shown in Fig. 5(b), (d), and (f). Owing to smaller core diameters and larger pump fluence in capillaries *I* and *II*, the emission spikes with FWHM around 0.5 nm were excited at relatively low pump energy so that we could not measure spontaneous emission. The intensity of lasing peak increased linearly with pump energy that could be linearly fitted (red line) and attributed to the stimulated emission. For the capillary *IV* (50 μm core diameter), the peak intensity of emission spike increased slowly with pulse energy at lower excitation, but enhanced dramatically as E_P above the certain threshold. After linear fitting, two red lines with different slopes were obtained to show the spontaneous emission and the stimulated emission at lower and higher excitation, respectively. Besides, the FWHM (blue solid circles) of emission spike decreased from 9.13 nm at $E_p = 5$ μJ/pulse to about 0.96 nm at $E_p = 30$ μJ/cm^2 in Fig. 5(f). In addition, the position of the slope efficiency variation and the occurrence of the narrower emission spikes were at the same pump energy of about 20 μJ/pulse.

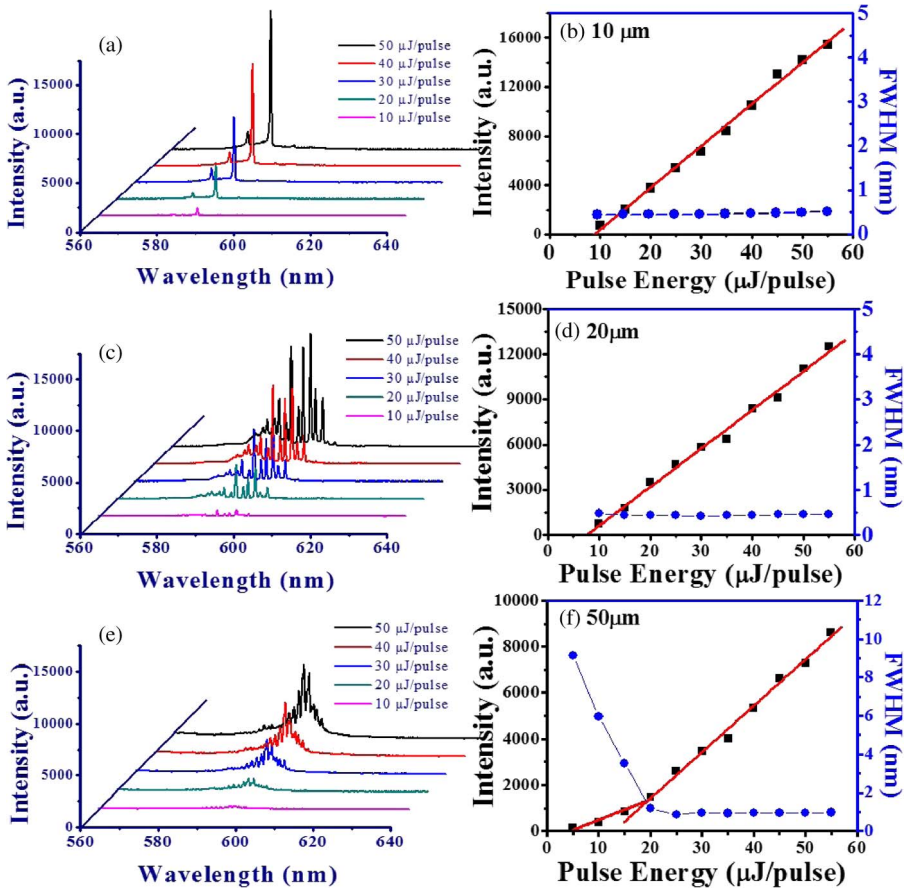

Fig. 5. Evolution of the emission spectra of DDLCs inside the single core capillary with core diameter of (a) 10 μm (capillary *I*), (c) 20 μm (capillary *II*), and (e) 50 μm (capillary *IV*) as pump energy (E_p) increased from 10 μJ/pulse to 50 μJ/pulse; the peak intensity and FWHM of emission spikes as a function of the pump energy from (b) capillary *I*, (d) capillary *II*, and (f) capillary *IV*.

Finally, we investigated the influence of working temperature on the lasing characteristics of DDLCs inside the capillary *II*, as shown in Fig. 6. Because the light scattering from LCs is mainly due to the intrinsic birefringence, the ratio for the amplitude of emission spikes to the spontaneous emission spectrum became unapparent and the emission spike revealed broadened FWHM at higher temperature above 45 °C. As the temperature decreased, the intensity of emission spikes increased owing to the enhancement of birefringence from LCs. Then, recurrent multiple light scattering would greatly enhance to result in light localization [28]. The emission spikes reveal the highest intensity and the shortest FWHM of about 0.468 nm with the temperature at the 20 °C in Fig. 6. However, the intensity of emission peaks decreased and linewidth of emission spike broadened again at even lower temperature (10 °C). It is recognized that the alignment of LCs became relative regular and thus light scattering decreased. Table 2 lists the peak wavelength (λ_p), FWHM ($\Delta\lambda$) and estimated Q-factor at different temperature. Due to the shortest FWHM of the emission peak about 0.468 (nm) at 20 °C, the estimated highest Q-factor is about 1273.8. The linewidth of emission spike broadens at higher or lower working temperatures and the estimated values of Q-factor are about 704.4 and 589.3 at 10 °C and 45 °C, respectively.

4. Conclusion

In summary, we investigate the random lasing characteristics from dye-doped nematic liquid crystals (E7) infilling of single core capillaries with four different core diameters. From the image

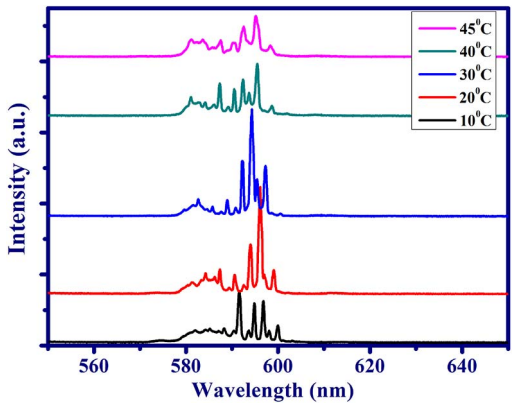

Fig. 6. Evolution of emission spectra of the DDLCs inside the single core capillary (capillary *II*) as the working temperature increases from 10 °C to 45 °C.

TABLE 2

Peak wavelength (λ_p), FWHM, and estimated Q-factor of the emission spectrum from the DDLCs inside capillary II at different temperatures

Temperature($^\circ C$)	10	15	20	25	30	35	40	45
Peak wavelength (nm)	591.7	596.9	596.1	595.2	594.3	595.5	595.5	595.2
FWHM (nm)	0.840	0.670	0.468	0.510	0.506	0.642	0.759	1.010
Q-factor,($\lambda_p/\Delta\lambda$)	704.4	891.0	1273.8	1167.1	1174.5	927.5	784.6	589.3

of polarization optical microscopy, the directors of NLCs inside capillary are shown to approximately along the axial direction but with slight disordering that will cause recurrent multiple light scattering. Through longitudinal pump by a frequency-doubling Q-switched Nd:YAG laser, light diffusion within NLCs would be effectively suppressed to produce light localization. Thus, several emission spikes with sub-nanometer linewidth can be excited above broad spontaneous emission spectrum. Unlike a large core diameter capillary with a number of the excited modes, only three emission spikes were excited from a capillary with 10 μm core diameter. However, the intensity of emission spike relative to the amplitude of spontaneous emission decreases and the emission linewidth (FWHM) broadens from larger core diameter capillary owing to the decrease of pump fluence and the increase of scattering loss. We also alter the emission spectrum of the random laser from a 20 μm core diameter capillary by means of temperature. The lasing emission spike reveals higher intensity and narrower FWHM of about 0.468 nm as temperature decreases to about 20 °C due to the increment of LC birefringence and enhancement of light scattering. With even lower temperature, the intensity of emission spikes decreases, and the FWHM broadens again because the LCs alignment inside capillary became relative ordering. The tunable emission spectrum of random laser opens up several applications, such as biological remote sensing.

References

[1] V. Letokhov, "Quantum statistics of multi-mode radiation form an ensemble of atoms," *Zk. Eksp. Teor. Fiz*, vol. 53, pp. 2210–2222, 1968.
[2] B. Redding, M. A. Choma, and H. Cao, "Speckle-free laser imaging using random laser illumination," *Nat. photon.*, vol. 6, no. 6, pp. 355–359, 2012.
[3] R. C. Polson and Z. V. Vardeny, "Random lasing in human tissues," *Appl. Phys. lett.*, vol. 85, no. 7, pp. 1289–1291, Aug. 2004.
[4] N. M. Lawandy, R. Balachandran, A. Gomes, and E. Sauvain, "Laser action in strongly scattering media," *Nature*, vol. 368, no. 6470, pp. 436–438, Mar. 1994.
[5] H. Cao *et al.,* "Random laser action in semiconductor powder," *Phys. Rev. Lett.*, vol. 82, no. 11, p. 2278, Mar. 1999.

[6] F. Chen and J.-M. Nunzi, "Distributed feedback laser action in reflection geometry from a dye-doped polymer film," *Opt. Mater.*, vol. 34, no. 8, pp. 1415–1418, Jun. 2012.
[7] D. S. Wiersma, "The physics and applications of random lasers," *Nat. Phys.*, vol. 4, no. 5, pp. 359–367, May 2008.
[8] D. Zhang, G. Kostovski, C. Karnutsch, and A. Mitchell, "Random lasing from dye doped polymer within biological source scatters: The pomponia imperatorial cicada wing random nanostructures," *Organic Electron.*, vol. 13, no. 11, pp. 2342–2345, Nov. 2012.
[9] Q. Song *et al.,* "Random lasing in bone tissue," *Opt. Lett.*, vol. 35, no. 9, pp. 1425–1427, May 2010.
[10] H. Cao, J. Xu, E. Seelig, and R. Chang, "Microlaser made of disordered media," *Appl. Phys. Lett.*, vol. 76, no. 21, pp. 2997–2999, 2000.
[11] C. Vanneste and P. Sebbah, "Localized modes in random arrays of cylinders," *Phys. Rev. E*, vol. 71, no. 2, 2005, Art. ID. 026612.
[12] G. Van Soest, M. Tomita, and A. Lagendijk, "Amplifying volume in scattering media," *Opt. Lett.*, vol. 24, no. 5, pp. 306–308, Mar. 1999.
[13] P. Sebbah and C. Vanneste, "Random laser in the localized regime," *Phys. Rev. B, Condens. Matter*, vol. 66, no. 14, 2002, Art. ID. 144202.
[14] H. Fujiwara, Y. Hamabata, and K. Sasaki, "Numerical analysis of resonant and lasing properties at a defect region within a random structure," *Opt. Exp.*, vol. 17, no. 5, pp. 3970–3977, Mar. 2009.
[15] Q. Song *et al.,* "Unidirectional high intensity narrow-linewidth lasing from a planar random microcavity laser," *Phys. Rev. Lett.*, vol. 96, no. 3, 2006, Art. ID. 033902.
[16] A. Vasdekis, G. Town, G. Turnbull, and I. Samuel, "Fluidic fibre dye lasers," *Opt. Exp.*, vol. 15, no. 7, pp. 3962–3967, Jan. 2007.
[17] C. J. de Matos *et al.,* "Random fiber laser," *Phys. Rev. Lett.*, vol. 99, no. 15, 2007, Art. ID. 153903.
[18] S. Gottardo, S. Cavalieri, O. Yaroshchuk, and D. S. Wiersma, "Quasi-two-dimensional diffusive random laser action," *Phys. Rev. Lett.*, vol. 93, no. 26, 2004, Art. ID. 263901.
[19] S. M. Morris *et al.,* "Electrically switchable random to photonic band-edge laser emission in chiral nematic liquid crystals," *Appl. Phys. Lett.*, vol. 100, no. 7, 2012, Art. ID. 071110.
[20] A. Ghasempour Ardakani, S. M. Mahdavi, and A. R. Bahrampour, "Tuning of random lasers by means of external magnetic fields based on the Voigt effect," *Opt. Laser Technol.*, vol. 47, pp. 121–126, Apr. 2013.
[21] Q. Song, L. Liu, L. Xu, Y. Wu, and Z. Wang, "Electrical tunable random laser emission from a liquid-crystal infiltrated disordered planar microcavity," *Opt. Lett.*, vol. 34, no. 3, pp. 298–300, Feb. 2009.
[22] C.-R. Lee *et al.,* "All-optically controllable random laser based on a dye-doped polymer-dispersed liquid crystal with nano-sized droplets," *Opt. Exp.*, vol. 18, no. 3, pp. 2406–2412, Feb. 2010.
[23] D. S. Wiersma and S. Cavalieri, "Light emission: A temperature-tunable random laser," *Nature*, vol. 414, no. 6865, pp. 708–709, Dec. 2001.
[24] J.-H. Lin, P.-Y. Chen, and J.-J. Wu, "Mode competition of two bandedge lasing from dye doped cholesteric liquid crystal laser," *Opt. Exp.*, vol. 22, no. 8, pp. 9932–9941, Apr. 2014.
[25] D. Luo *et al.,* "Temperature effect on the lasing from a dye-doped two-dimensional hexagonal photonic crystal made of holographic polymer-dispersed liquid crystals," *J. Appl. Phys.*, vol. 108, no. 1, 2010, Art. ID. 013106.
[26] F. Yao *et al.,* "Polarization and polarization control of random lasers from dye-doped nematic liquid crystals," *Opt. Lett.*, vol. 38, no. 9, pp. 1557–1559, May 2013.
[27] Y. Liu, X. Sun, H. Elim, and W. Ji, "Gain narrowing and random lasing from dye-doped polymer-dispersed liquid crystals with nanoscale liquid crystal droplets," *Appl. Phys. Lett.*, vol. 89, no. 1, 2006, Art. ID. 011111.
[28] J.-H. Lin and Y.-L. Hsiao, "Manipulation of the resonance characteristics of random lasers from dye-doped polymer dispersed liquid crystals in capillary tubes," *Opt. Mater. Exp.*, vol. 4, no. 8, pp. 1555–1563, Aug. 2014.
[29] L. Li and L. Deng, "Random lasers in dye-doped polymer-dispersed liquid crystals containing silver nanoparticles," *Physica B: Condensed Matter*, vol. 407, no. 24, pp. 4826–4830, Dec. 2012.
[30] L. Li, L. Wang, and L. Deng, "Low threshold random lasing in DDPDLCs, DDPDLC @ ZnO nanoparticles and dye solution @ ZnO nanoparticle capillaries," *Laser Phys. Lett.*, vol. 11, no. 2, 2014, Art. ID. 025201.